Mechanical, Physical and Thermal Properties of Polylactic Acid Filament Composite Reinforced with Newly Isolated *Cryptostegia grandiflora* Fiber

Udhayakumar Arumaiselvan,[a] Mayandi Kalimuthu,[a] Rajini Nagarajan,[a,*] Murali Mohan,[b] Sikiru O. Ismail,[c] Faruq Mohammad,[d] Hamad A. Al-Lohedan,[d] and Kumar Krishnan [e]

By leveraging the properties of natural or plant fibers and possibilities through three-dimensional (3D) printing technology, a composite filament was fabricated by incorporating newly isolated *Cryptostegia grandiflora* fiber (CGF), as a reinforcement with polylactic acid (PLA) by using a twin-screw extruder. The fabricated composite filament and pure PLA filament were 3D-printed, using fused deposition modeling (FDM). This study investigated the mechanical, physical, and thermal properties of the 3D-printed CGF reinforced composite filament samples. The mechanical properties of the samples fabricated with 10 wt% CGF were better than that of samples with pure PLA. In addition, impact, tensile, flexural strengths and hardness were increased by 35.6, 33.6, 14.1, and 1.7%, respectively, when compared with the sample with pure PLA. The fractured surface morphology of tensile samples showed a uniform distribution of CGF within the PLA. The addition of CGF improved the thermal stability of the 3D-printed CGF/PLA composite sample by 15%. Therefore, the printed structure could serve as an alternative material for various uses, considering contemporary concepts of sustainability, availability, environmental friendliness, and cost effectiveness.

DOI: 10.15376/biores.19.2.3740-3754

Keywords: Natural fiber; Cryptostegia grandiflora filler; Polylactic acid; Additive manufacturing; 3D printing; Mechanical properties; Zero waste; Sustainability label

*Contact information: a: Department of Mechanical Engineering, School of Mech, Auto, Aero and Civil Engineering, Kalasalingam Academy of Research and Education, Anandnagar, Krishnankoil, Virudhunagar Dt., India; b: Department of Science and Technology, Kalasalingam Academy of Research and Education, Anandnagar, Krishnankoil, Virudhunagar Dt., India; c: Department of Engineering, Center for Engineering Research, University of Hertfordshire, Hatfield, Hertfordshire AL10 9AB, England, United Kingdom; d: Department of Chemistry, College of Science, King Saud University, Riyadh 11451, Kingdom of Saudi Arabia; e: Faculty of Health and Life Sciences, INTI International University, Persiaran Perdana BBN, 71800 Nilai, Negeri Sembilan, Malaysia; * Corresponding author: rajiniklu@gmail.com*

INTRODUCTION

Additive manufacturing (AM) technology is used to create three-dimensional (3D) objects by adding successive layers of materials. Compared to conventional manufacturing methods, AM has many advantages, including the possibility to produce complex shaped objects with high quality and low material waste. Therefore, AM is an excellent choice for developing functional prototypes (Kain *et al*. 2020). In AM technologies, fused deposition modelling (FDM) is one of the most widely used methods, due to cost-effectiveness, ease of use, and large build volumes, among others.

In the FDM process, filaments made of thermoplastic polymers, such as poly lactic acid (PLA), polyethylene terephthalate glycol (PETG), and acrylonitrile butadiene styrene (ABS) are used (Liu *et al*. 2019). Thermoplastic, as a filament, is used in FDM to produce various automobile components, to contribute to other industrial applications, and to prepare structures for buildings (Cantrell *et al*. 2017). The use of thermoplastics with higher melting temperatures as 3D printing materials has recently become possible (Wu *et al*. 2015). Due to its high mechanical properties, stability, and biological origin, PLA polymer is one of the most used materials in 3D printing (Serra *et al*. 2013). At the same time, PLA has drawbacks, including low impact strength and high brittleness. To overcome the limitations of PLA, addition of fibers or fillers to PLA can be expected to strengthen its physical, mechanical, and thermal properties (Bajpai *et al*. 2013; Li *et al*. 2016).

Based on previous studies, composites containing fine fibers have dominated the production of plastics for the past 50 years. Natural fibers have been used as reinforcement in some composites due to their availability, cost-effectiveness, environmental friendliness, and good mechanical, physical, and thermal characteristics. But, the drawback of natural fiber includes their hydrophilic nature. When natural fiber is used as reinforcement in hydrophobic polymer, the interfacial adhesion between fiber and polymer may suffer due to interfacial incompatibility. This leads to reduced mechanical properties of the composite. To overcome this problem, many studies have used chemical treatments on natural fibers. Alkaline treatment is commonly used to reduce the hydrophilic properties of natural fibers; in addition, the size of the particles used as reinforcement can have a significant effect on the interfacial adhesion between fiber and polymer (Aida *et al.* 2021; Mocanu *et al*. 2022).

Manufacturing companies, such as Toyota, Volvo, Audi, and BMW utilize natural fiber reinforced polymer composite filaments to manufacture automotive interior parts. Moreover, it is evident that these filaments are beneficial for the production of intricate and real automotive interior components, using additive manufacturing techniques (Ahmad *et al*. 2014; Balla *et al*. 2019; Tezara *et al.* 2022; Nazir *et al*. 2023). The demand for 3D printing is also increasing; therefore, there is increased scholarly interest in natural fiber reinforced PLA filament used in 3D printing (Ambone *et al*. 2020; Zhao *et al*. 2022).

A natural fiber was isolated for the first time from the *Cryptostegia grandiflora* plant. The origin of the plant is southwest Madagascar, and the plant has spread worldwide. The plant can grow up to 30 meters with support. The chemical composition of *Cryptostegia grandiflora* fibers (CGFs) has been found to be similar to other natural fibers, such as sisal, jute, hemp, and bamboo (Udhayakumar *et al*. 2023). A detailed analysis of literature review results indicates that when 10 wt% natural filler is reinforced into the polymer matrix, the most favorable results are achieved in the mechanical and thermal properties of the composite. This finding shows the importance of selecting and finalizing the matrix ratio for optimal composite performance (Aggarwal *et al*. 2019; Sekar *et al*. 2021; Gauss *et al*. 2022; Scaffaro *et al*. 2022; Khan *et al*. 2023).

In this study, CGF/PLA composite filament with 10 wt% CGF was fabricated using a twin-screw extruder and used for 3D printing. The effect of adding CGFs to PLA on the thermal and mechanical properties of FDM 3D-printed samples was investigated. Also, a scanning electron microscope (SEM) was used to study the morphology of the 3D-printed samples.

EXPERIMENTAL

Materials

A newly extracted CG fiber was used as a reinforcement. The fiber extraction and characterization have been carried out and previously reported (Udhayakumar *et al*. 2023). Poly(lactic acid) pellets with a weight average molecular weight of 6.7 x 10^4 g/mol and a density of 1.2 g/cm^3 were used as the matrix. The glass transition and melting temperatures of PLA were 59 and 143 °C, respectively.

Methods

Composite filament production

The CG fiber was cut into small pieces with a length of 10.0 ± 0.5 mm. Then, 30 g of the pieces were placed in a beaker and immersed in a 10% KOH solution for about 4 h. The treated CG fiber was heated in a water bath at 90 °C for 1 h. Once the heat treatment was completed, the CG fiber was allowed to cool to a room temperature. The fiber was incubated in a hot air oven at 60 °C for 2 h. The dried fibers were then ground into powder. The powder thus prepared was referred to as filler in the production of filament. To create the CGF/PLA filament, a twin-screw extruder (Brabender, Duisburg, Germany) with a screw diameter of 32 mm and a L/D ratio of 16:1 was used for the melt extrusion. The optimal temperature for smooth extrusion and optimum filament diameter was determined to be between 170 and 200 °C. Therefore, the extrusion temperature was controlled within that range and a filament with a diameter of 1.75 ± 0.05 mm was produced.

Printing parameters

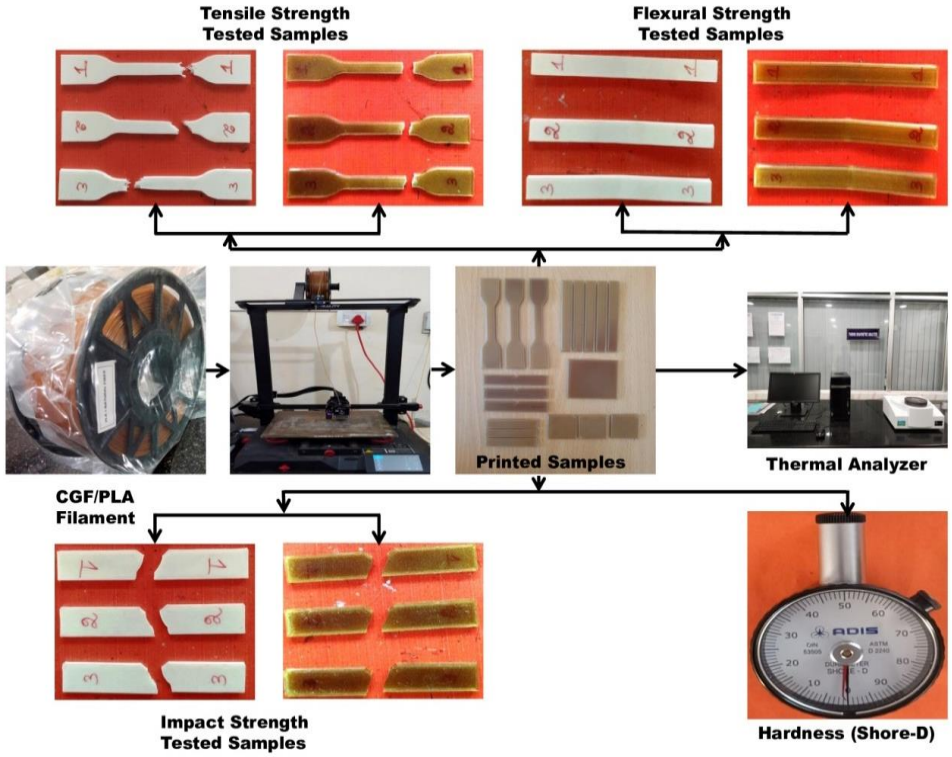

Fig. 1. Schematic diagram of the process adopted

The schematic diagram of the whole process is shown in Fig. 1. The diameter of the fabricated CGF/PLA composite filament was 1.75 ± 0.05 mm. The test parts were created using a 3D printer of fused deposition modeling (CREALITY SERMOON D1) with 0.4 mm nozzle diameter. The printing parameters used to fabricate the samples in FDM 3D printer are presented in Table 1.

Table 1. 3D Printing Process Parameters

Parameter	Description
Filament diameter (mm)	1.75 ± 0.05
Nozzle diameter (mm)	0.4
Layer height (mm)	0.1
Printing bed temperature (°C)	60
PLA filament printing nozzle temperature (°C)	190
CGF + PLA filament printing nozzle temperature (°C)	205
PLA filament printing speed (mm/sec)	45
CGF + PLA filament printing speed (mm/sec)	35

Density

According to ASTM D792 (2020), an analytical balance (Sartorius Quintix 124-1 S) was used to weigh the samples in both air and water. The experimental density (ρ_{exp}) was determined, using Eq. 1,

$$\rho_{exp} = \frac{W_a - W_w}{W_a} x\ \rho_w \quad (1)$$

where W_a refers to the weight of the sample in air, W_w denotes the weight of the sample in water, and ρ_w stands for the density of water.

Tensile test

The samples for the tensile tests were prepared using ASTM D638 TYPE IV (2014), with specimen dimensions specified as 115 mm × 19 mm × 3 mm. A universal testing machine was used, with a load capacity of 10 kN and a constant feed rate of 5 mm/min. Three printed samples for both filaments were tested, and the average value was reported.

Flexural test

The samples for the flexural testing were prepared, according to ASTM D790 (2017). A flexural testing machine with a load capacity of 10kN at a rate of 5 mm/min was used. The specimen dimensions are 125 mm × 13 mm × 3 mm. Three samples were tested, and the average value was reported, in order to ensure the accuracy of the results.

Impact test

The Izod test apparatus was used to determine the impact strength of the composite in accordance with ASTM D256 (2023). The specimen dimensions are 65 mm × 13 mm × 3 mm. In each group three samples were subjected to impact tests, and the average result was reported.

Hardness test

The hardness of the samples was determined by using the shore D hardness machine (ADIS Durometer Shore-D). Measurements of the samples were calculated on the Shore-D scale in accordance with the ASTM D2240 (2015) standard, utilizing specimens sized 20 mm x 20 mm x 3 mm. For each sample, indentations were made in five distinct locations, and the average hardness value was recorded.

Scanning electron microscope

Scanning electron microscope (SEM; CARL ZEISS SEM SIGMA) was used to investigate the morphology of the samples at 20 kV. The sample was gold-coated before SEM examination. The cross-section of the fractured tensile test samples was used to examine the microstructure of the composite.

Thermal analysis

Thermal stability of 3D-printed CGF/PLA composite was investigated, using thermogravimetric analysis (TGA); model STA8000 according to ASTM E1131 (2020). The sample was tested from 40 to 600 °C at a heating rate of 5 °C/min and a nitrogen flow of 20 mL/min.

Water absorption

The water absorption behaviors of pure PLA and 10 wt% CGF/PLA filament printed sample were measured at a room temperature, considering the ASTM D570 (2022) standard. The sample was dried for 8 h in a hot air oven at 50 °C before the water absorption test. Afterwards, the sample was immersed in deionized water after the initial weight was measured. The sample weight was then measured every 24 h for 360 h and calculated as follows,

$$W_A = \frac{W_2 - W_1}{W_1} x\ 100 \quad (2)$$

where W_A refers to the weight percentage of the sample, W_1 indicates the initial weight of the sample, and W_2 denotes the weight of the sample after immersion.

RESULTS AND DISCUSSION

Density

The density of a composite material is an important factor to determine the properties of the composite. It depends on the proportions of both reinforcement and matrix in the composite. The densities of CGF, PLA, and 10% CGF/PLA filament were 1.020, 1.230, and 1.166 g/cm^3, respectively. When adding CGF as a reinforcement to PLA, the density of the fabricated composite filament was decreased by 6%. Perhaps the ligno-cellulosic fibers' closed morphology and lower density of CG fiber caused to the decreased density of the PLA (Kariz *et al*. 2018; Mazur *et al*. 2022).

Tensile test

To investigate the effect of CGF on PLA, tensile strength, and elongation at break were measured on 3D-printed samples of PLA and CGF/PLA composite.

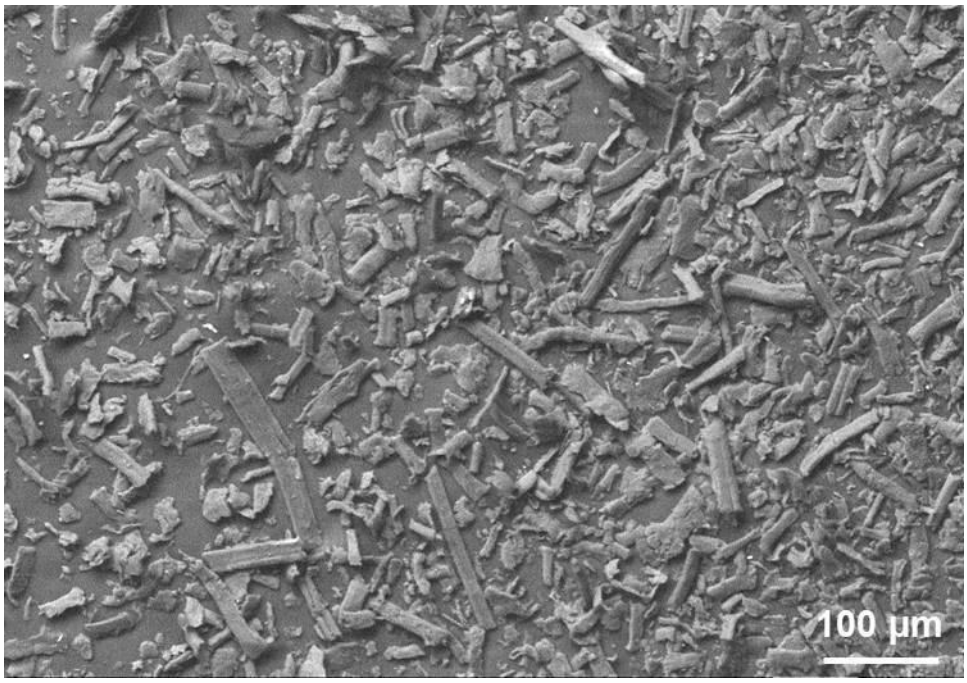

Fig. 2. SEM image of CG powder

The tensile strengths of both CGF/PLA composite and pure PLA are shown in Fig. 3. Due to the addition of filler, the 3D-printed CGF/PLA composite recorded higher tensile strength than pure PLA, but it had lower elongation at break. The addition of 10 wt% of CGF increased the tensile strength of the 3D-printed sample by 33.6%. The treatment of the surface of fibers and the size of reinforcement were found to be important factors that influenced the adhesion between the reinforcement and the matrix. Figure 2 shows that more than 70% of the particles were less than 100 µm in size.

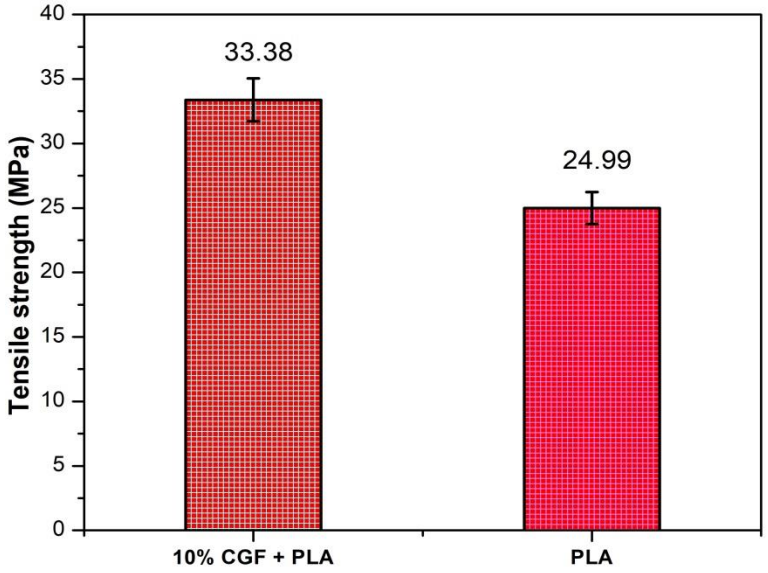

Fig. 3. Tensile strengths of PLA and 10 wt% CGF/PLA filament composite (Error bar represents 95% confidence interval of the mean)

As these micron size fillers were well integrated into the polymer matrix, a strong bond was formed between the filler and the matrix (Fu *et al*. 2008; Mocanu *et al*. 2022; Scaffaro *et al*. 2022). The high tensile strength at 10 wt% can be attributed to the uniform dispersion of CGF particles in the PLA matrix and good interfacial adhesion between CGF particles and PLA matrix, as subsequently confirmed with SEM and elucidated. This resulted in a high stress transfer from the PLA matrix to the CGF particles (Kakroodi *et al*. 2014). The elongation of the PLA and 10 wt% CGF/PLA filament printed samples were 7.4% and 6.33%, respectively. Notably, the elongation at break decreased by 16.9% with addition of filler. This was attributed to the fact that fibers with high cellulose content are brittle and stiff. Hence, they acted as stress concentrators in the polymer matrix, reducing the elongation of the composite (Ambone *et al*. 2020).

Flexural Test

The natural fibers commonly act as a rigid filler to increase the stiffness of polymer matrix and establish a strong bond with the PLA matrix. Figure 4 depicts the flexural strength values of pure PLA and CGF/PLA composite. The flexural strength of CGF/PLA composite was higher than pure PLA by 14.1%. The increased flexural strength was mostly due to the interfacial adhesion between the fiber and matrix as well as the cellulose content of the filler (Nishino *et al*. 2003; Huda *et al*. 2008). The improved flexural characteristics are appropriate for high bending strength applications.

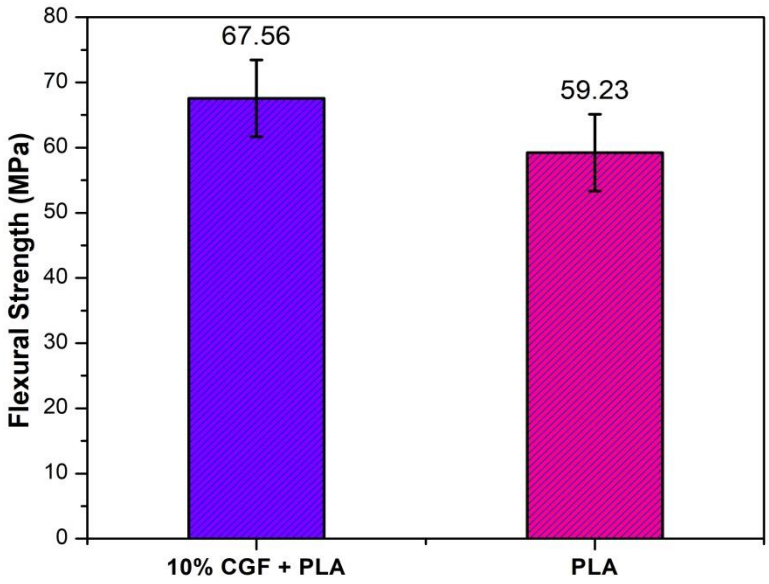

Fig. 4. Flexural strengths of PLA and 10 wt% CGF/PLA filament composite (Error bar represents 95% confidence interval of the mean.)

Impact Test

The composition of fiber, such as cellulose, lignin, and others influences the impact strength of a composite. Figure 5 shows that the impact resistance of PLA matrix sample was improved by adding fillers. When compared to pure PLA samples, the CGF/PLA composite sample exhibited the maximum impact strength of 3.43 kJ/m^2. The improved impact strength was due to the interfacial bonding between the PLA matrix and CGF (Kumar *et al*. 2022).

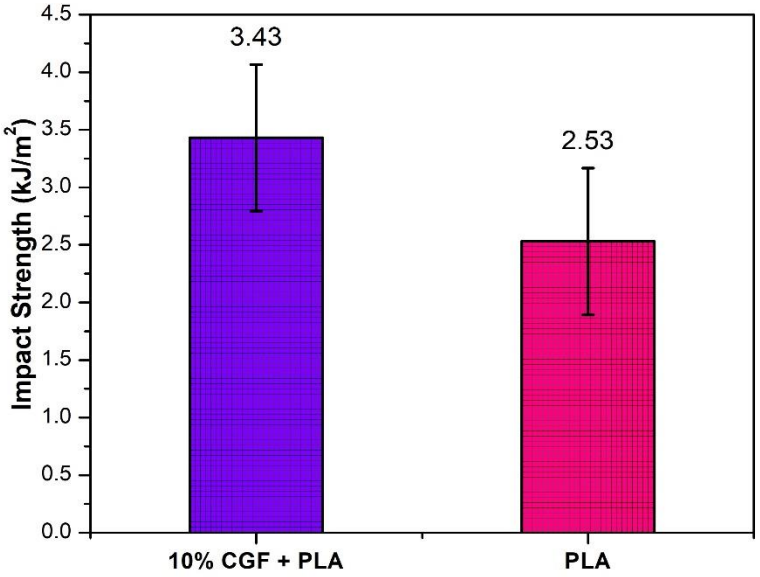

Fig. 5. Impact strengths of PLA and 10 wt% CGF/PLA filament composite (Error bar represents 95% confidence interval of the mean.)

Hardness Test

Figure 6 depicts a comparison of hardness test results. The hardness of the 3D-printed CGF/PLA composite sample increased due to the plant fiber reinforcement in the PLA matrix. Among the tested samples, the average hardness value for CGF/PLA composite was 83.0 (Shore-D) and that of pure PLA sample was 81.6 (Shore-D). One of the primary concerns was that the composite material became more brittle when it was harder, as similarly studied by Felix Sahayaraj *et al*. (2022).

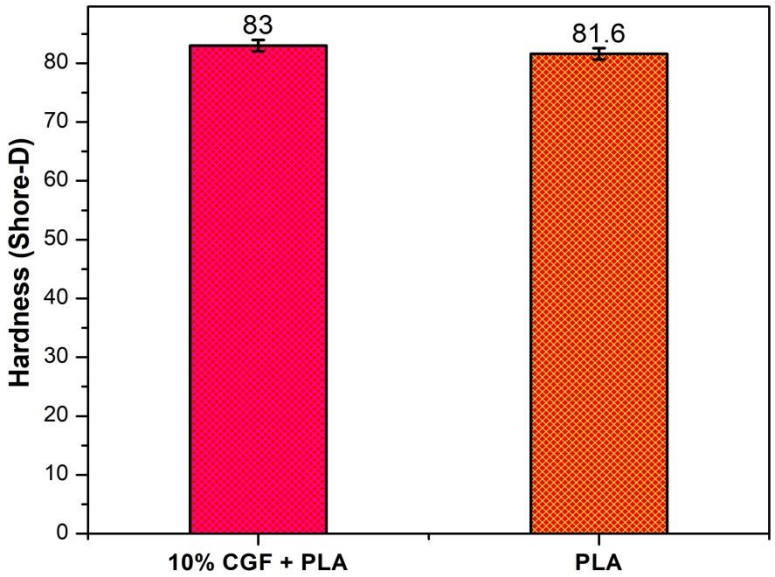

Fig. 6. Hardness of PLA and 10 wt% CGF/PLA filament composite (Error bar represents 95% confidence interval of the mean.)

SEM Analysis

The morphology of the tensile fractured surfaces of both PLA and CGF/PLA composite samples are shown in Fig. 7. The fillers were separated from one another during the extrusion process and were well-dispersed in the PLA matrix, as observed in Figs. 7(b) and (c). There were some voids on the fractured surface. This is attributed to the fillers being trapped in the PLA matrix. Using micron size fillers enhanced the performance of the filler-reinforced PLA composites. The increased surface area of micron size fillers allowed better accessibility of functional groups on the filler surface, which promoted extensive hydrogen bonding with the PLA matrix. This strong bonding led to an improved adhesion between the fillers and the matrix. The bridging effect could help to reduce crack development and allow for effective stress transfer between the matrix and the fillers, which is expected to result in an enhanced mechanical tensile property (Cheng *et al*. 2009). In Fig. 7(d), the fillers were broken along with the PLA matrix. This provides evidence that the CGF had good adhesion with the PLA matrix.

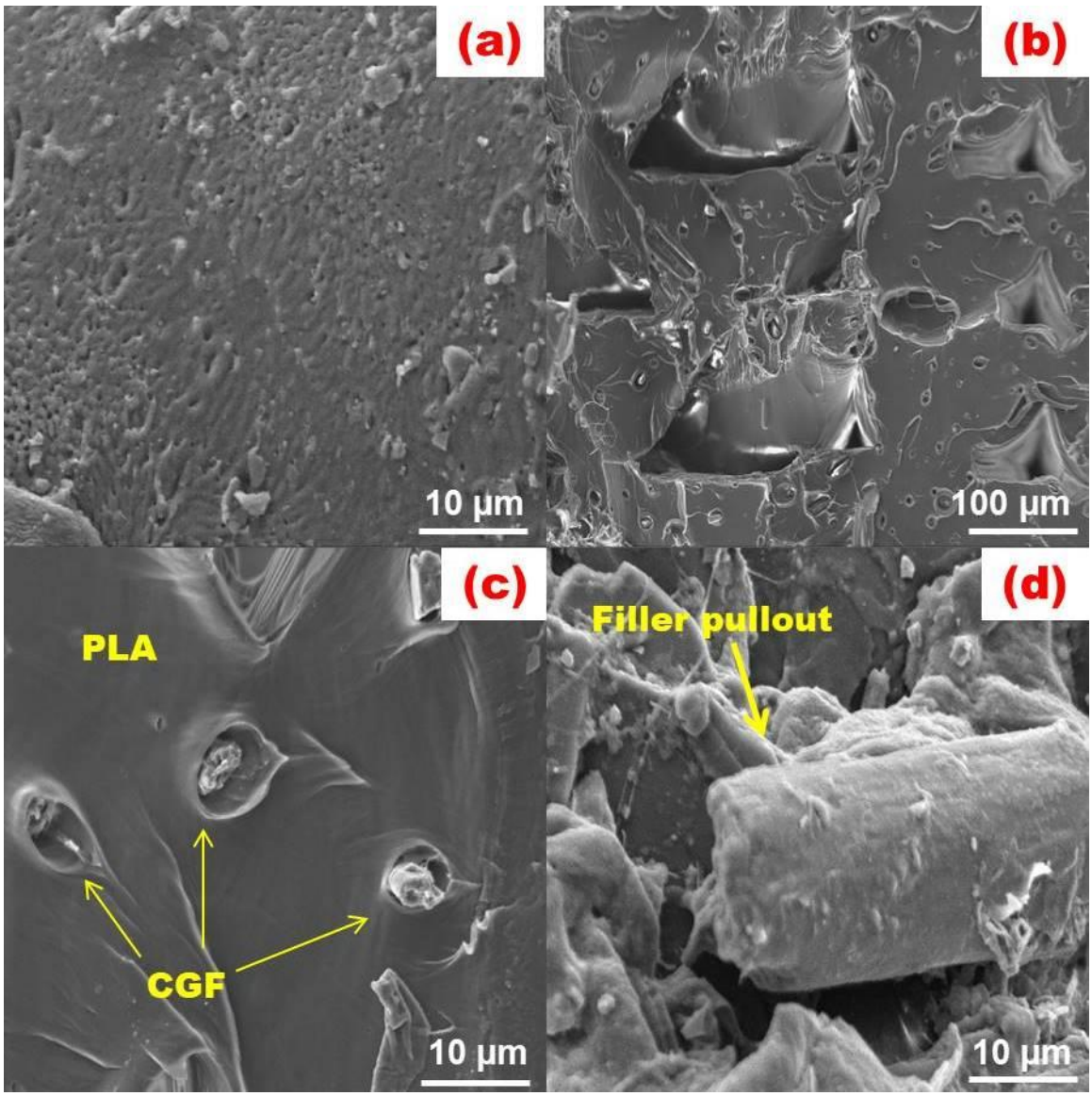

Fig. 7. SEM images of (a) Pure PLA (b - d) 10 wt% CGF/PLA filament composite

Thermal Analysis

Figure 8 depicts the thermogravimetric curves for the pure PLA and 10% CGF, respectively. The analysis of thermogravimetric curves indicated the degree of thermal stability and degradation kinetics of the additively manufactured composite sample, when subjected to higher temperatures. The minor weight loss between 100 and 200 °C in all the samples was attributed to the desiccation of trapped and bound water from composite material as well as the evaporation of moisture present in the sample (Carrete *et al*. 2019; Chakraborty and Biswas 2020).

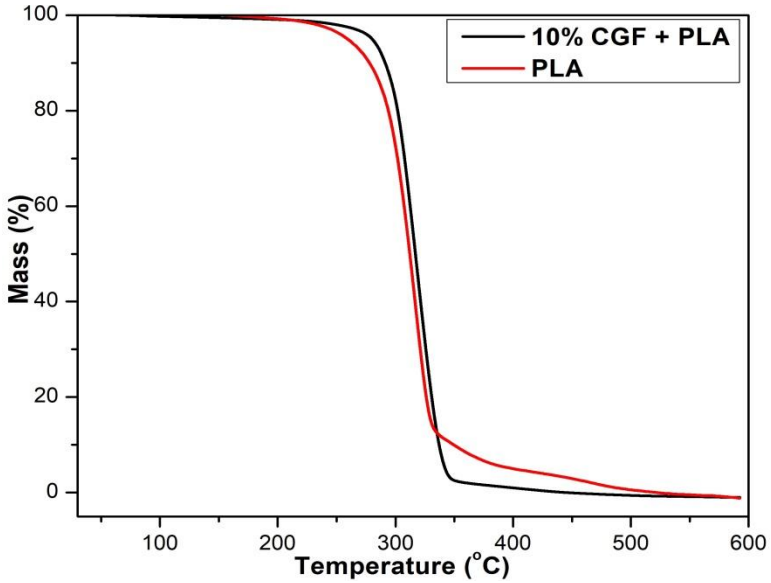

Fig. 8. TGA curves of PLA and 10 wt% CGF/PLA filament composite

The TGA curves show a single decomposition step for the samples, with the main decomposition having occurred between 230 and 350 °C. The major weight loss was due to the decomposition of lignin, hemicellulose, and cellulose, which are the molecules present in CGF within the following temperature ranges: 160 to 900, 220 to 315, and 315 to 400 °C, respectively (Yang *et al*. 2007; Mu *et al*. 2014c; Feng *et al*. 2019; Kamarudin *et al*. 2019). The initial decomposition temperatures of PLA and CGF reinforced samples were 230 and 265 °C, respectively. Addition of CGF to PLA increased the thermal stability of the composites by 15%. The results implied that 3D-printed CGF/PLA sample possessed a good thermal stability up to a temperature of nearly 200 °C and without degradation.

Water Absorption

The percentage weight gain of PLA and 10 wt% CGF/PLA filament printed samples in distilled water for 360 h at 24-h intervals is shown in Fig. 9. After the test for 360 h, the neat PLA showed water absorption of 1.89%, indicating its hydrophobic nature. The weight gain percentage of the 10 wt% CGF/PLA filament sample was 2.07%. The average weight percentage of the CGF/PLA filament sample was 9.52% higher than that of the PLA filament sample. This suggested that CGF/PLA filament had less water resistance than PLA filament, due to the hydrophilic nature of CG fiber. The FTIR study also confirmed that CGF contained a significant number of hydrophilic OH groups, as previously investigated (Udhayakumar *et al*. 2023). The water absorption of the samples varied up to 312 h; afterwards the water absorption of the samples remained constant until

360 h, which is similar to reported studies (Sanadi *et al*. 1995; Nair *et al*. 2018). The results of this study can support the development of useful products for various sectors, such as aerospace, automotive and construction industries.

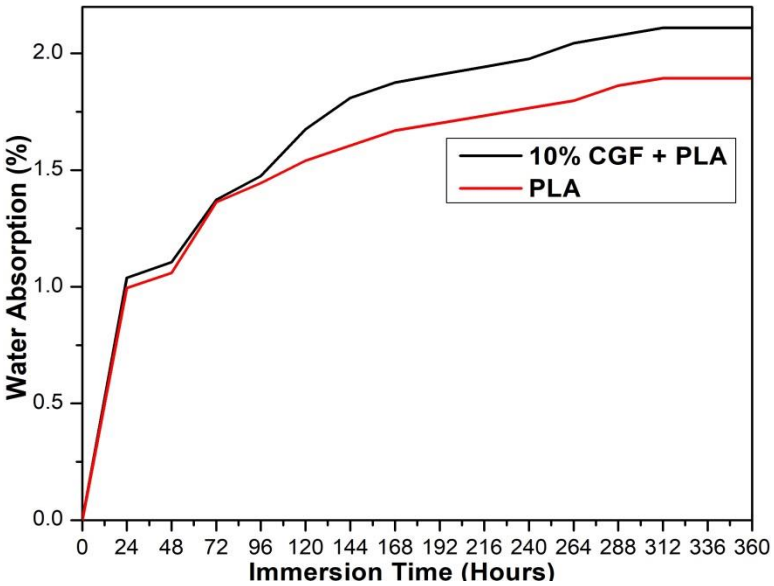

Fig. 9. Water absorption behaviors of PLA and 10 wt.% CGF/PLA filament composite

CONCLUSIONS

1. Fused deposition modeling (FDM) technology was used to print *Cryptostegia grandiflora* fiber/poly(lactic acid) (CGF/PLA) filament and additively manufactured green composite samples.
2. The addition of CGF enhanced the mechanical characteristics of the 3D-printed composite samples.
3. From the experimental results obtained, it was evident that strong interfacial adhesion between reinforcement and matrix of the samples improved their tensile, flexural, impact strengths, and toughness.
4. According to scanning electron microscopic (SEM) images, CGFs were observed to be uniformly distributed in the PLA matrix. Furthermore, the thermogravimetric analysis (TGA) results indicated that the 10 wt% CGF/PLA composite recorded better thermal stability than pure PLA. Also, adding CGF filler to PLA reduced the density of the composite, leading to lighter weight composite products.

ACKNOWLEDGEMENTS

The KSU authors acknowledge the funding from Researchers Supporting Project number (RSP2024R355), King Saud University, Riyadh, Saudi Arabia. Also, this work is a part of the Department of Science and Technology (DST) - Science for Equity, Empowerment and Development (SEED) Division - Science, Technology and Innovation

(STI) Hub Project with DST File No: DST/SEED/SCSP/STI/2019/127. Therefore, the authors sincerely thank the DST for the approval of the project and Kalasalingam Academy of Research and Education for their support, allowing the research to be successfully conducted in their laboratories.

REFERENCES CITED

Aggarwal, S., Johnson, S., Saloni, D., and Hakovirta, M. (2019). "Novel 3D printing filament composite using diatomaceous earth and polylactic acid for materials properties and cost improvement," *Composites Part B: Engineering* 177. DOI: 10.1016/j.compositesb.2019.107310

Ahmad, F., Choi, H. S., and Park, M. K. (2014). "A review: Natural fiber composites selection in view of mechanical, light weight, and economic properties," *Macromolecular Materials and Engineering* 300(1), 10–24. DOI: 10.1002/mame.201400089

Aida, H., Nadlene, R., Mastura, M. T., Yusriah, L., Malingam, S. D., and Ilyas, R. A. (2021). "Natural fibre filament for fused deposition modelling (FDM): A review," *International Journal of Sustainable Engineering* 14(6), 1988-2008. DOI: 10.1080/19397038.2021.1962426

Ambone, T., Torris, A., and Shanmuganathan, K. (2020). "Enhancing the mechanical properties of 3D printed polylactic acid using nanocellulose," *Polymer Engineering and Science* 60(8), 1842–1855. DOI: 10.1002/pen.25421

ASTM D638 (2014). "Standard test method for tensile properties of plastics," ASTM International, West Conshohocken, PA, USA.

ASTM D2240 (2015). "Standard test method for rubber property-durometer hardness," ASTM International, West Conshohocken, PA, USA.

ASTM D790 (2017). "Standard test methods for flexural properties of unreinforced and reinforced plastics and electrical insulating materials," ASTM International, West Conshohocken, PA, USA.

ASTM D792 (2020). "Standard test methods for density and specific gravity (Relative density) of plastics by displacement," ASTM International, West Conshohocken, PA, USA.

ASTM E1131 (2020). "Standard test methods for compositional analysis by thermogravimetry," ASTM International, West Conshohocken, PA, USA.

ASTM D570 (2022). "Standard test method for water absorption of plastics," ASTM International, West Conshohocken, PA, USA.

ASTM D256 (2023). "Standard test methods for determining the Izod pendulum impact resistance of plastics," ASTM International, West Conshohocken, PA, USA.

Bajpai, P. K., Singh, I., and Madaan, J. (2013). "Tribological behavior of natural fiber reinforced PLA composites," *Wear* 297(1–2), 829–840. DOI: 10.1016/j.wear.2012.10.019

Balla, V. K., Kate, K. H., Satyavolu, J., Singh, P., and Tadimeti, J. G. D. (2019). "Additive manufacturing of natural fiber reinforced polymer composites: Processing and prospects," *Composites Part B: Engineering* 174, article 106956. DOI: 10.1016/j.compositesb.2019.106956

Cantrell, J. T., Rohde, S., Damiani, D., Gurnani, R., DiSandro, L., Anton, J., Young, A., Jerez, A., Steinbach, D., Kroese, C., and Ifju, P. G. (2017). "Experimental

characterization of the mechanical properties of 3D-printed ABS and polycarbonate parts," *Rapid Prototyping Journal* 23(4), 811–824. DOI: 10.1108/RPJ-03-2016-0042

Carrete, I. A., Bermudez, D., Aguirre, C., Alvarez-Primo, F. A., Anil-Kumar, S., Chinolla, P., Gamboa, M., Gonzalez, S. A., Heredia, H. E., Hernandez, A. M., Levario, E., Lindquist, J. R., Luna, V. C., Martinez, L. M., Mendez, V. E., Slager, J. J., Ugarte-Sanchez, L., Urquidi, Y. A., Zamora, A., and Roberson, D. A. (2019). "Failure analysis of additively manufactured polyester test specimens exposed to various liquid media," *Journal of Failure Analysis and Prevention* 19(2), 418–430. DOI: 10.1007/s11668-019-00614-0

Chakraborty, S., and Biswas, M. C. (2020). "3D printing technology of polymer-fiber composites in textile and fashion industry: A potential roadmap of concept to consumer," *Composite Structures* DOI: 10.1016/j.compstruct.2020.112562

Cheng, S., Lau, K. tak, Liu, T., Zhao, Y., Lam, P. M., and Yin, Y. (2009). "Mechanical and thermal properties of chicken feather fiber/PLA green composites," *Composites Part B: Engineering*, 40(7), 650–654. DOI: 10.1016/j.compositesb.2009.04.011

Felix Sahayaraj, A., Muthukrishnan, M., and Ramesh, M. (2022). "Experimental investigation on physical, mechanical, and thermal properties of jute and hemp fibers reinforced hybrid polylactic acid composites," *Polymer Composites* 43(5), 2854–2863. DOI: 10.1002/pc.26581

Feng, X., Wu, Z., Xie, Y., and Wang, S. (2019). "Reinforcing 3D print methacrylate resin/cellulose nanocrystal composites: Effect of cellulose nanocrystal modification," *BioResources* 14(2), 3701–3716. DOI: 10.15376/biores.14.2.3701-3716

Fu, S., Feng, X., Lauke, B., and Mai, Y. (2008). "Effects of particle size, particle/matrix interface adhesion and particle loading on mechanical properties of particulate–polymer composites," *Composites Part B: Engineering* 39(6), 933-961. DOI: 10.1016/j.compositesb.2008.01.002

Gauss, C., Pickering, K. L., Tshuma, J., and McDonald-Wharry, J. (2022). "Production and assessment of poly(lactic acid) matrix composites reinforced with regenerated cellulose fibres for fused deposition modelling," *Polymers* 14(19). DOI: 10.3390/polym14193991

Huda, M. S., Drzal, L. T., Mohanty, A. K., and Misra, M. (2008). "Effect of fiber surface-treatments on the properties of laminated biocomposites from poly(lactic acid) (PLA) and kenaf fibers," *Composites Science and Technology* 68(2), 424–432. DOI: 10.1016/j.compscitech.2007.06.022

Kain, S., Ecker, J. V., Haider, A., Musso, M., and Petutschnigg, A. (2020). "Effects of the infill pattern on mechanical properties of fused layer modeling (FLM) 3D printed wood/polylactic acid (PLA) composites," *European Journal of Wood and Wood Products* 78(1), 65–74. DOI: 10.1007/s00107-019-01473-0

Kakroodi, A. R., Cheng, S., Sain, M., and Asiri, A. (2014). "Mechanical, thermal, and morphological properties of nanocomposites based on polyvinyl alcohol and cellulose nanofiber from *Aloe vera* rind," *Journal of Nanomaterials* 2014, Article no. 903498. DOI: 10.1155/2014/903498

Kamarudin, S. H., Abdullah, L. C., Aung, M. M., and Ratnam, C. T. (2019). "Mechanical and physical properties of kenaf-reinforced poly(lactic acid) plasticized with epoxidized jatropha oil," *BioResources* 14(4), 9001-9020. DOI: 10.15376/biores.14.4.9001-9020

Kariz, M., Sernek, M., Obućina, M., and Kuzman, M. K. (2018). "Effect of wood content in FDM filament on properties of 3D printed parts," *Materials Today Communications* 14, 135–140. DOI: 10.1016/j.mtcomm.2017.12.016

Khan, I., Neeraj kumar, Yadav, J. S., Choudhary, M., Chauhan, A., and Singh, T. (2023). "Utilization of waste slate powder in poly(lactic acid) based composite for 3D printer filament," *Journal of Materials Research and Technology* 24, 703–714. DOI: 10.1016/j.jmrt.2023.03.046

Kumar, R. P., Muthukrishnan, M., and Sahayaraj, A. F. (2022). "Experimental investigation on jute/snake grass/kenaf fiber reinforced novel hybrid composites with *Annona reticulata* seed filler addition," *Materials Research Express* 9(9). DOI: 10.1088/2053-1591/ac92ca

Li, N., Li, Y., and Liu, S. (2016). "Rapid prototyping of continuous carbon fiber reinforced polylactic acid composites by 3D printing," *Journal of Materials Processing Technology* 238, 218–225. DOI: 10.1016/j.jmatprotec.2016.07.025

Liu, Z., Wang, Y., Wu, B., Cui, C., Guo, Y., and Yan, C. (2019). "A critical review of fused deposition modeling 3D printing technology in manufacturing polylactic acid parts," *International Journal of Advanced Manufacturing Technology*, Springer London. DOI: 10.1007/s00170-019-03332-x

Mazur, K. E., Borucka, A., Kaczor, P., Gądek, S., Bogucki, R., Mirzewiński, D., and Kuciel, S. (2022). "Mechanical, thermal and microstructural characteristic of 3D printed polylactide composites with natural fibers: Wood, bamboo and cork," *Journal of Polymers and the Environment* 30(6), 2341–2354. DOI: 10.1007/s10924-021-02356-3

Mocanu, A.-C., Miculescu, F., Dascălu, C.-A., Voicu, Ștefan I., Pandele, M.-A., Ciocoiu, R., Batalu, D., Dondea, S., Mitran, V., and Ciocan, L. T. (2022). "Influence of ceramic particles size and ratio on Surface—Volume features of the naturally derived HA-Reinforced filaments for biomedical applications," *Journal of Functional Biomaterials* 13(4), 199. DOI: 10.3390/jfb13040199

Mu, C., Xue, L., Zhu, J., Jiang, M., and Zhou, Z. (2014b). "Mechanical and thermal properties of toughened Poly(L-lactic) acid and lignin blends," *BioResources* 9(3), 5557-5566. DOI: 10.15376/biores.9.3.5557-5566

Nair, M. M., Shetty, N., Divakara, S. S., and Kamath, S. (2018). "Effect of distilled and sea water absorption on mechanical behaviour of short coir fibre epoxy composite/sawdust filler," *Pertanika J. Sci. & Technol*, 26(1), 261-282.

Nazir, M. H., Al-Marzouqi, A. H., Ahmed, W., and Zaneldin, E. (2023). "The potential of adopting natural fibers reinforcements for fused deposition modeling: Characterization and implications," *Heliyon* 9(4), article e15023. DOI: 10.1016/j.heliyon.2023.e15023

Nishino, T., Hirao, K., Kotera, M., Nakamae, K., and Inagaki, H. (2003). "Kenaf reinforced biodegradable composite," *Composites Science and Technology* 63(9), 1281–1286. DOI: 10.1016/S0266-3538(03)00099-X

Sanadi, A. R., Daniel Caulfield, gt F., Jacobson, R. E., and Rowelltg, R. M. (1995). "Renewable Agricultural Fibers as Reinforcing Fillers in Plastics: Mechanical Properties of Kenaf Fiber-Polypropylene Composites," *Ind. Eng. Chem. Res* 34(5), 1889-1896. DOI: 10.1021/ie00044a041

Scaffaro, R., Citarrella, M. C., Catania, A., and Settanni, L. (2022). "Green composites based on biodegradable polymers and anchovy (*Engraulis encrasicolus*) waste suitable for 3D printing applications," *Composites Science and Technology* 230. DOI: 10.1016/j.compscitech.2022.109768

Sekar, V., Zarrouq, M., and Namasivayam, S. N. (2021). "Development and characterization of oil palm empty fruit bunch fibre reinforced polylactic acid filaments for fused deposition modeling," *Journal of Mechanical Engineering* 18(1), 89–107.

Serra, T., Planell, J. A., and Navarro, M. (2013). "High-resolution PLA-based composite scaffolds via 3-D printing technology," *Acta Biomaterialia* 9(3), 5521–5530. DOI: 10.1016/j.actbio.2012.10.041.

Tezara, C., Siregar, J. P., Hamdan, M. H. M., Rihayat, T., Bachtiar, D., Fitriyana, D. F., and Prayitno, P. (2022). Influence of layering sequences on tensile properties of hybrid woven Jute/Ramie fibre reinforced polyester composites. *Materials Today: Proceedings* 48, 1836-1841. DOI: 10.1016/j.matpr.2021.09.151.

Udhayakumar, A., Mayandi, K., Rajini, N., Devi, R. K., Muthukannan, M., and Murali, M. (2023). "Extraction and characterization of novel natural fiber from *Cryptostegia grandiflora* as a potential reinforcement in biocomposites," *Journal of Natural Fibers* 20(1). DOI: 10.1080/15440478.2022.2159607

Wu, W., Geng, P., Li, G., Zhao, D., Zhang, H., and Zhao, J. (2015). "Influence of layer thickness and raster angle on the mechanical properties of 3D-printed PEEK and a comparative mechanical study between PEEK and ABS," *Materials* 8(9), 5834–5846. DOI: 10.3390/ma8095271

Yang, H., Yan, R., Chen, H., Lee, D. H., and Zheng, C. (2007). "Characteristics of hemicellulose, cellulose and lignin pyrolysis," *Fuel* 86(12–13), 1781–1788. DOI: 10.1016/j.fuel.2006.12.013

Zhao, G., Liu, H. Y., Cui, X., Du, X., Zhou, H., Mai, Y. W., Jia, Y. Y., and Yan, W. (2022). "Tensile properties of 3D-printed CNT-SGF reinforced PLA composites," *Composites Science and Technology* 230. DOI: 10.1016/j.compscitech.2022.109333

Article submitted: December 19, 2023; Peer review completed: February 11, 2024; Revised version received: March 25, 2024; Accepted: April 22, 2024; Published: April 25, 2024.
DOI: 10.15376/biores.19.2.3740-3754